Sol-gel synthesis of Al-Tin oxide thin films deposited via dip-coating technique

A. Ammari [1,2,*]
[1)] *Department of Physics, Faculty of Matter Sciences, University of Tiaret, (Algeria).*
[2)] *Laboratory of Micro and Nanophysics, National Polytechnic School of Oran (ENPO), Algeria.*

[*] Email address : ammari.hoss@gmail.com

***Abstract* — Thin films of Al-doped SnO_2, have been synthesized via sol-gel method and deposited by the dip-coating technique. The samples were characterized by UV-visible spectroscopy, Fourier transform infrared spectroscopy, and impedance spectroscopy, respectively. The effect of thermal annealing and Al-doping on the optoelectronic properties, were investigated. The Nyquist plots suggest that the conduction in the films is correlated with the formation of oxygen vacancies and the scattering of charge carriers over the grains boundaries.**

Keywords* — *Thin films, Al-doped SnO_2, sol-gel, impedance spectroscopy.

I. Introduction

SnO_2 thin films have potential applications in the areas of solar cells [1], gas sensor materials [2], catalysis [3], architectural windows [4] and optoelectronic devices (light emitting diodes [5] and transparent field effect transistors [6]. High quality thin films are indispensable for the optoelectronic devices. In this respect, SnO_2 is a material of choice owing to its wider optical transparency than many other metal oxide semiconductors with ~ 80% in the visible range [7]. SnO_2 exists in the tetragonal rutile crystal (SG: P42/mnm) [8] with a band gap of ~ 3.6 eV. The performance of devices based SnO_2 is known to strongly depend on the transportation over the grains and grains boundaries [9]. The present study, deals with the characteristics of the electrical conduction. The effect of Al-doping on both the optical and electrical properties of the films is investigated.

II. Experimental Details

The films were deposited by dip-coating technique on glass subtracts (Silicon subtracts were used for the infrared measurements). The sol-gel solutions were synthesized from ($SnCl_2.2H_2O$), $AlCl_3.6H_2O$ as dopant precursor ([Al]/[Sn]) and anhydrous ethanol (C_2H_5OH). The dopant concentrations were 2.5, 5 and 10% wt. After drying, the amorphous films were introduced in pre-heated oven at 500 °C, for 15 min. Fig 1 shows the steps during the sol-gel synthesis of the films.

The optical transmission of thin films was recorded at room temperature by a dual beam UV–Vis spectrophotometer (UV-1650 Shimadzu) in the range (280 – 1000 nm). The FTIR spectra of the samples were collected using Alpha Bruker ATR-spectrometer in the range (400–4000 cm^{-1}). The impedance measurements, were performed using Agilent 4284A LCR-meter.

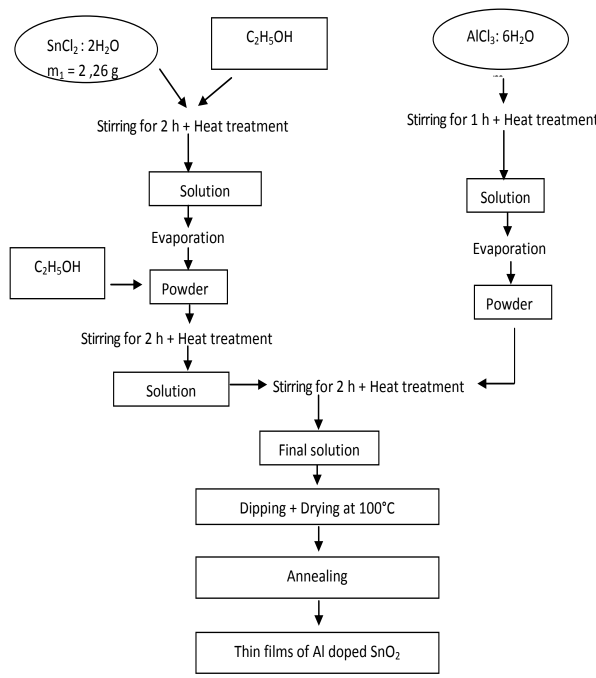

Fig. 1: Sol–gel synthesis of Al-doped SnO_2 thin films.

III. Results and Discussions

A. UV visible spectroscopy

Fig. 2 displays the UV-Vis spectra of the films deposited with different parameters. It is observed that the films exhibit a high transparency (T ~ 85 %) over the visible region, attributed to a decrease of the scattering effects and a better structural homogeneity.

In the strong absorption region, the optical band gap (Eg) is deduced from the Tauc plot: $(\alpha h\nu)^2$ vs. $h\nu$. Tables below summarizes the obtained optical band gap and the results of the conductivity tests.

The results show a red-shift consistent with introduction of electronic states in the bulk associated to both Sb-doping

A. Ammari (ammari.hoss@gmail.com).

and oxygen defects. The width of the band tails of the localized states in presence of inhomogeneous disorder.

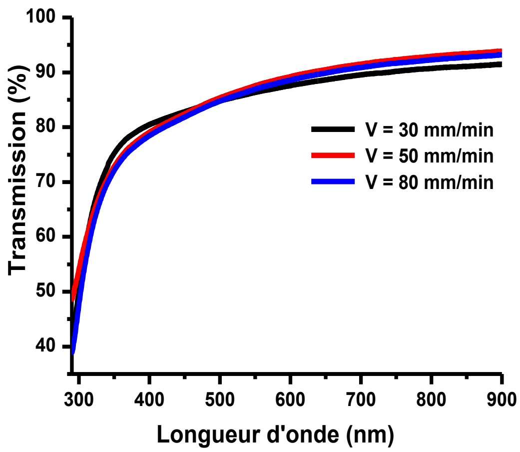

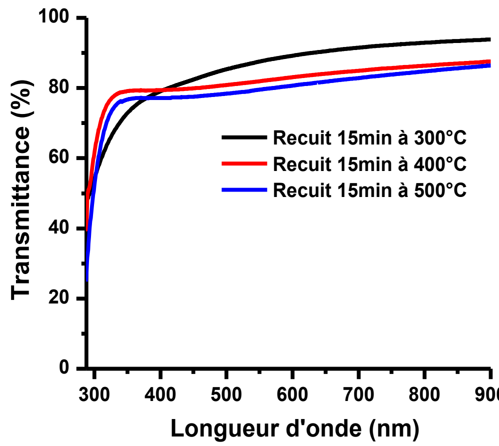

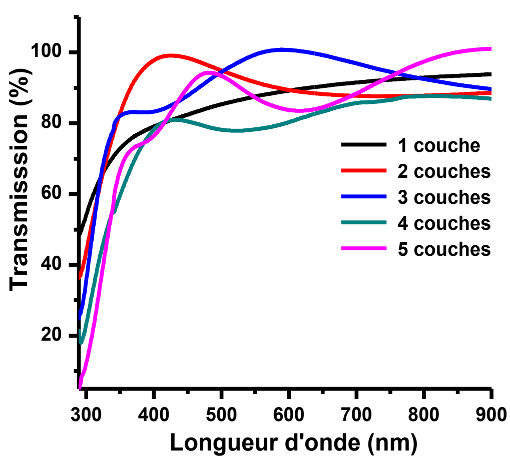

Fig. 2: UV-visible spectra of Al-doped SnO_2 thin films.

B. FTIR spectroscopy

Fig. 2 shows the infrared transmission spectra of Al-doped SnO_2, deposited by dip-coating on silicon substrates and annealed at 500 ° C for two hours.

Film	Parameters	Gap	Conductivity
V = 30 mm/min	Drying : 15 min/100 °C	3.96	Weak
V = 50 mm/min	Annealing : 15 min/500 °C	3.86	Good
V = 80 mm/min		3.95	Weak

Table 1: Films deposited at different speeds.

V = 50 mm/min			
Film	**Parameters**	**Gap**	**Conductivity**
Annealing 15 min/300°C	Drying :	4.121	Insulator
Annealing 15 min/400°C	15 min/100°C	4.232	Weak
Annealing 15 min/500°C		3.857	Good

Table 2: Films annealed at different temperatures for 15 min.

V = 50 mm/min			
Film	**Parameters**	**Gap**	**Conductivity**
1 C	Deposit- Drying- Annealing	3.855	Good
2 C		3.903	Good
3 C	Drying 15 min/100 °C Annealing 15 min/500 °C	3.981	Good
4 C		3.901	Weak
5 C		3.923	Weak

Table 4: Films annealed at 500 °C for 15 min.

The typical Sn-O-Sn vibrations appear in the range of 737 cm^{-1}. The band at 895 cm^{-1} is probably the absorption peaks of the Al-O metal hydroxyl groups [6,7]. The peak at 613 cm^{-1} is attributed to the stretching vibration mode of Sn-O bonds which are optical active phonon modes in infrared [8]. We observe the deformation bands of C=O around 1120 cm^{-1}. Also, the presence of OH groups is confirmed through the broad bands around 2600 cm-1 and 2325 cm^{-1} [9]. We suggest that the origin of these connections is due to the solvents involved in the protocol and the water (H_2O) absorbed after deposition.

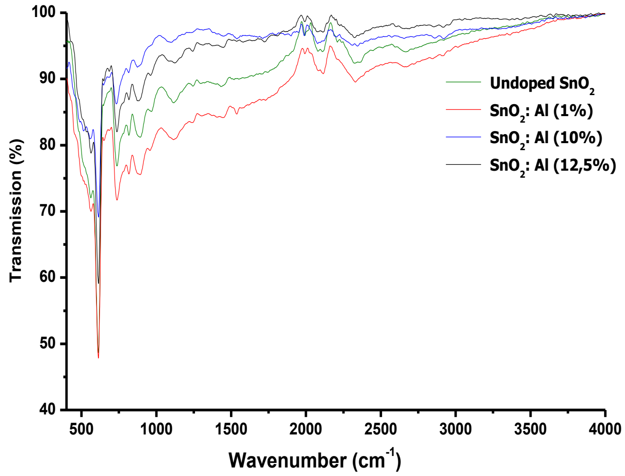

Fig. 3. FTIR-ATR transmission spectra of Al-doped SnO_2 thin films.

C. Impedance spectroscopy

The impedance spectroscopy is a method for characterizing the electrical properties of materials and their interfaces with electrically conductive electrodes. In order to get satisfying measurements, we deposited aluminum barrette as ohmic contacts by vacuum evaporation.

Fig. 4 is the Nyquist representation of undoped tin oxide thin films. We note that the equivalent circuit for each sample is an RC circuit on parallel [15]. This allows us to say that the type of circuit is not affected by the number of layers, however, the resistance R shifted to larger values. The frequency varies from 75 kHz to 30 MHz recorded at room temperature.

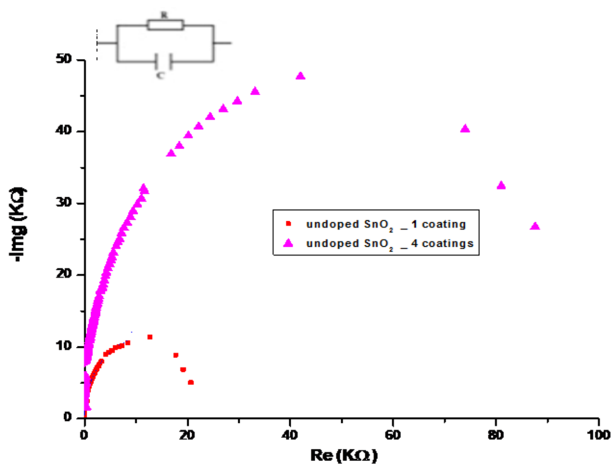

Fig. 4. The Nyquist representation for undoped layer and four layers.

The maximum of the imaginary part is moved from 11.3 to 47.7 KΩ, i.e. to larger values. Moreover, the cut-off frequency, which corresponds to the maximum, is shifted to lower frequencies. We calculated the capacitance C for each sample [16]. Table 2 shows the values obtained for the undoped Tin oxide SnO_2 films. The measured resistances and capacitances may be attributed to grain boundaries between nanocrystals and seems to be a consequence of orderedness/crystallization of the film, whereas the rise of resistance may be related with the reduction of carrier density through trapping of electrons at grain boundaries by adsorbed oxygen during annealing in air.

Fig. 5 shows the Nyquist representation of SnO_2 thin films for different rate of doping. The resistance increases with the increase of the dopant content and reaches a value of 27.7 kΩ for a doping rate of 12.5% Al and the capacity decreases to a value of 8.26 pF for the same rate of doping by aluminum.

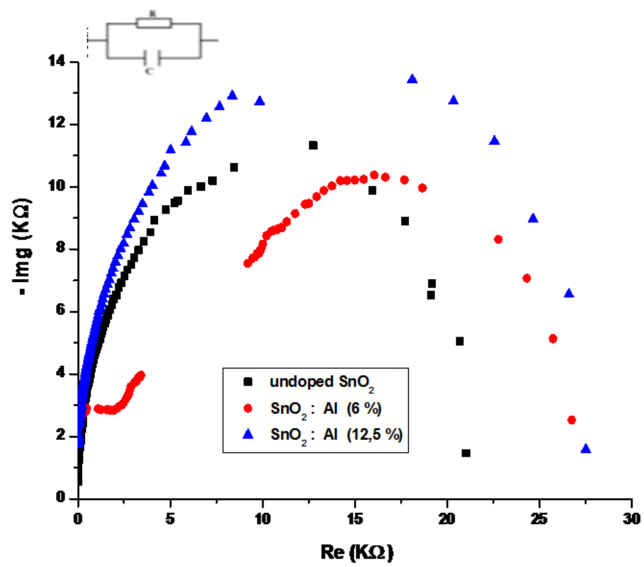

Fig. 5. The Nyquist representation of Al-doped SnO_2 thin films.

The change in capacitance is connected with the formation of oxygen vacancies due to the substitution of Sn^{4+} by Al or Al^{3+} ions on the surface of grains. A high concentration of vacancies in the surface of the grains is a continuous path for the charge carriers through the layer of Al-doped Tin oxide. The increase of the electric resistance can be attributed to the segregation at the crystallite boundary, which has been attributed to a change in carrier mobility. So the impedance results show quantitatively the important contribution of the grain or crystallite boundary potential in the electrical resistance of SnO_2 thin films.

IV. Conclusion

In this work, we have investigated the optical and the electrical properties of Al-doped SnO_2 thin films. We have found that the optical band gag is about 3.8 – 4.3 eV. The conductivity depends strongly on the conditions during deposition and thermal annealing. The impedance spectroscopy shows that the electrical conductivity of the film is determined by charge transport through the interface of the crystallites and that the effect of crystallite boundary potential becomes more dominant through doped layers.

REFERENCES

[1] F. Cai, Z. Yuan, Y. Duan, L. Bie, TiO2 coated SnO2 nanosheet films for dye-sensitized solar cells, Thin Solid Films 519 (2011) 5645–5648.

[2] S. Nardis, D. Monti, C. Di Natale, A. D'Amico, P. Siciliano, A. Forleo, M. Epifani, A. Taurino, R. Rella, R. Paolesse, Preparation and characterization of cobalt porphyrin modified tin dioxide films for sensor applications, Sensor. Actuat. B 103 (2004) 339–343.

[3] A. Bhattacharjee, M. Ahmaruzzaman, T. Sinha, A novel approach for the synthesis of SnO2 nanoparticles and its application as a catalyst in the reduction and photo-degradation of organic compounds, Spectrochimica Acta A 136 (2015) 751–760.

[4] B.G. Lewis, D.C. Paine, Applications and processing of transparent conducting oxides, MRS Bull. 25 (2000) 22-27.

[5] D. Vaufrey, M.B. Khalifa, M.P. Besland, C. Sandu, M.G. Blanchin, V. Teodorescu, J.A. Roger, J. Tardy, Reactive ion etching of sol–gel-processed SnO2 transparent conducting oxide as a new material for organic light emitting diodes, Synthetic Metals 127 (2002) 207–211.

[6] R.E. Presley, C.L. Munsee, C.H. Park, D. Hong, J.F. Wager, D.A. Keszler, Tin oxide transparent thin film transistors, J. Phys. D 37 (2004) 2810.

[7] A. Ammari, B. Bellal, N. Zebbar, B. Benrabah, M. Trari, Thermal-frequency dependence study of the sub-band localized states effect in Sb-doped SnO2 based sol-gel thin films, Thin Solid Films 632 (2017) 66-72.

[8] R. K. Sonker, A. Sharma, M. Shahabuddin, M.Tomar, V. Gupta, Low temperature sensing of NO2 gas using SnO2-ZnO nanocomposite sensor. Adv. Mat. Lett, 4 (2013) 196-201.

[9] E. A. Morais, L. V. D. A. Scalvi, V. Geraldo, S. J. L. Ribeiro, C. V. Santilli, Er rare-earth ion incorporation in sol-gel SnO2. Mater. Res. 6 (2003) 445-449.

[10] R. D. Tarey and T. A. Raju, "A method for the deposition of transparent conducting thin films of tin oxide," *Thin Solid Films*, vol. 128, no. 3–4, pp. 181–189, Jun. 1985.

[11] P. Barbarat, S. F. Matar, and G. Le Blevennec, "First-principles investigations of the electronic, optical and chemical bonding properties of SnO_2," *Journal of Materials Chemistry*, vol. 7, no. 12, pp. 2547–2550, 1997.

[12] T. Schuler and M. Aegerter, "Optical, electrical and structural properties of sol gel ZnO:Al coatings," *Thin Solid Films*, vol. 351, no. 1–2, pp. 125–131, Aug. 1999.

[13] M. Kojima, H. Kato and M. Gatto, Philos. Mag. B, 68 (2) (1993) 215-222.

[14] E. Shanti, V. Dutta, A. Banerjee and K.L. Chopra, J. Appl. Phys., 51 (12) (1980) 6243--6251.

[15] B. Gautheron, M. Labeau, G. Delabouglise, and U. Schmatz, "Undoped and Pd-doped SnO_2 thin films for gas sensors," *Sensors and Actuators B: Chemical*, vol. 16, no. 1–3, pp. 357–362, Oct. 1993.

[16] B. Benrabah, A. Bouaza, A. Kadari, and M. A. Maaref, "Impedance studies of Sb doped SnO_2 thin film prepared by sol gel process," *Superlattices and Microstructures*, vol. 50, no. 6, pp. 591–600, Dec. 2011.

[17] M.-R. Yang, S.-Y. Chu, R.-C. Chand, Sens. Actuators B, 122 (2007), p. 269.